Chaperone-like Activity of High-Mobility Group Box 1 Protein and Its Role in Reducing the Formation of Polyglutamine Aggregates

Hyun Jin Min,*,† Eun Ae Ko,*,† Jie Wu,*,† Eun Sung Kim,* Min Kyung Kwon,* Man Sup Kwak,* Ji Eun Choi,‡ Jong Eun Lee,†,§ and Jeon-Soo Shin*,†,¶,‖

High-mobility group box 1 protein (HMGB1), which mainly exists in the nucleus, has recently been shown to function as a sentinel molecule for viral nucleic acid sensing and an autophagy regulator in the cytoplasm. In this study, we studied the chaperone-like activity of HMGB1 and found that HMGB1 inhibited the chemically induced aggregation of insulin and lysozyme, as well as the heat-induced aggregation of citrate synthase. HMGB1 also restored the heat-induced suppression of cytoplasmic luciferase activity as a reporter protein in hamster lung fibroblast O23 cells with expression of HMGB1. Next, we demonstrated that HMGB1 inhibited the formation of aggregates and toxicity caused by expanded polyglutamine (polyQ), one of the main causes of Huntington disease. HMGB1 directly interacted with polyQ on immunofluorescence and coimmunoprecipitation assay, whereas the overexpression of HMGB1 or exogenous administration of recombinant HMGB1 protein remarkably reduced polyQ aggregates in SHSY5Y cells and *hmgb1*$^{-/-}$ mouse embryonic fibroblasts upon filter trap and immunofluorescence assay. Finally, overexpressed HMGB1 proteins in mouse embryonic primary striatal neurons also bound to polyQ and decreased the formation of polyQ aggregates. To this end, we have demonstrated that HMGB1 exhibits chaperone-like activity and a possible therapeutic candidate in polyQ disease. ***The Journal of Immunology*****, 2013, 190: 1797–1806.**

High-mobility group box 1 (HMGB1) is a highly conserved nuclear protein, and its amino acid sequence is conserved across species (1). In most eukaryotic cells, HMGB1 is located in the nucleus, where it functions as a nucleosome stabilizer and a regulator of transcription (2, 3). HMGB1 recently has been shown to play a role as a cytokine-like molecule when it is released into extracellular space. HMGB1 can be released passively after necrosis and also actively from macrophages and monocytes if they are stimulated (4). HMGB1 binds to TLR-2, -4, and receptor for advanced glycation end products (5, 6) and promotes inflammation. HMGB1 was also shown to act as a late mediator of endotoxemia and sepsis in animal models and human patients (7–10). HMGB1 moves to the cytoplasm via a redox-dependent mechanism and plays a role as a regulator between macroautophagy and apoptosis in the cytoplasm by binding to beclin-1 and dissociating from bcl-2 (11).

Some proteins form aggregates under stressful conditions such as increases of reactive oxygen species, metal ions, or aging (12–14). Aggregated proteins can be cleared by macroautophagy (15, 16), and chaperones are known to modify proteostasis strongly (17, 18). Polyglutamine (polyQ) tract is present in wild-type proteins that are from a cytosine-adenine-guanine (CAG) repeat coding for a glutamine. PolyQ expansion disease family includes at least nine heritable disorders of Huntington disease and the spinocerebellar ataxias SCA1, SCA2, SCA3, SCA6, SCA7, and SCA17 caused by expansion of a CAG repeat of affected proteins (19). Huntington disease is a neurodegenerative disorder caused by the aggregation of an expanded polyQ of the mutant huntingtin protein (mHtt) over 35 CAG repeats in the gene (20) and expanded polyQ tracts beyond the threshold influence on secondary structure and cause the formation of aggregates (21, 22). The aggregates formed by polyQ induce neuronal cell toxicity by several mechanisms such as proteasomal dysfunction (23) and sequestration of transcriptional factors (24). How the mutated proteins in these polyQ cause disease in cellular and molecular mechanisms is still in discussions; however, the clearance of aggregates formed by polyQ is a therapeutic target.

Molecular chaperones are defined as any protein that interacts with and stabilizes another protein to acquire its functionally active conformation, without being present in its final structure (25). Chaperones like HSP70 can suppress the formation of mHtt aggregates, alleviating its toxicity in cultured cells and animal models (26–28). Upregulation of chaperones such as HSP70 and HSP40 decrease the formation of aggregates, and, therefore, chaperone molecules have been considered as one of the therapeutic targets in many aggregate-prone diseases (29).

*Department of Microbiology, Yonsei University College of Medicine, Seoul 120-752, Korea; †Brain Korea 21 Project for Medical Science, Yonsei University College of Medicine, Seoul 120-752, Korea; ‡Department of Pediatrics, Seoul National University Boramae Hospital, Seoul National University College of Medicine, Seoul 110-799, Korea; §Department of Anatomy, Yonsei University College of Medicine, Seoul 120-752, Korea; ¶Severance Biomedical Science Institute, Yonsei University College of Medicine, Seoul 120-752, Korea; and ‖Institute for Immunology and Immunological Diseases, Yonsei University College of Medicine, Seoul 120-752, Korea

Received for publication September 4, 2012. Accepted for publication December 5, 2012.

This work was supported by grants from the National Research Foundation of Korea funded by the Korea government (Ministry of Education, Science and Technology) (2011-0017611), the Korean Healthcare technology R&D Project, Ministry of Health and Welfare (A101024), and the Brain Korea 21 Project for Medical Sciences, Republic of Korea.

Address correspondence and reprint requests to Prof. Jeon-Soo Shin, Department of Microbiology, Yonsei University College of Medicine, 50 Yonsei-ro Seodaemoon-gu, Seoul 120-752, Korea. E-mail address: jsshin6203@yuhs.ac

The online version of this article contains supplemental material.

Abbreviations used in this article: CAG, cytosine-adenine-guanine; HMGB1, high-mobility group box 1 protein; Htt, huntingtin; MEF, mouse embryonic fibroblast; mHtt, mutant huntingtin protein; NAC, *N*-acetyl-L-cysteine; PI, propidium iodide; PLA, proximity ligation assay; polyQ, polyglutamine; rHMGB1, recombinant high-mobility group box 1 protein; ROS, reactive oxygen species; RT, room temperature.

In the current study, we investigated the chaperone-like function of HMGB1 by applying physical stress to target proteins and intracytoplasmic stress to luciferase and polyQ proteins. We show that HMGB1 inhibits the chemically induced aggregation of insulin and lysozyme as well as the heat-induced aggregation of citrate synthase in vitro. In an in vivo refolding assay using hamster lung fibroblast O23 cells, HMGB1 also decreased the heat-induced inactivation of the luciferase protein. In an aggregation-prone model of expanded polyQ, we demonstrated that HMGB1 proteins could bind to polyQ and reduce the formation of aggregates, diminishing the cytotoxicity caused by polyQ aggregates.

Materials and Methods

Cell culture and DNA transfection

Human neuroblastoma cell line SHSY5Y, human embryonic kidney epithelial cells HEK293, hamster lung fibroblasts O23, mouse embryonic fibroblast (MEF) NIH3T3 cells, and *hmgb1*$^{-/-}$ MEF cells (HMGBiotech) were cultured at 37˚C under 5% CO_2 in DMEM supplemented with 10% FBS (Life Technologies), 100 U/ml penicillin, 100 μg/ml streptomycin, and 2 mM L-glutamine. The cells were transfected with polyQ and/or various HMGB1 plasmids with the aid of Lipofectamine 2000 (Invitrogen). Electroporation was used for transfection in MEF cells using a microporator (Invitrogen).

Human Htt plasmid (pcDNA3-Htt Ex1) containing exon 1 with 25 glutamine or 97 glutamine repeats followed by a GFP sequence (25Q-GFP or 97Q-GFP) (a kind gift from Dr. W.J. Park, Gwanju Institute of Science and Technology, Gwanju, South Korea) (30) was used for the aggregation study. Myc-tagged wild-type HMGB1 as well as HMGB1 boxes A (aa 1–79) and B (aa 88–162) plasmids were used for the transfection study (31, 32). We used recombinant HMGB1 (rHMGB1) proteins produced in insect High Five cells (Insect HMGB1; ATGen), a mouse myeloma cell line of NS0 (R&D Systems), or human cells (Euk HMGB1; Sino).

Measurement of chaperone-like activity of HMGB1 in vitro

A turbidity measurement was performed to measure the level of protein aggregation following a previous protocol with minor modifications (33). To check the chaperonic effect of HMGB1 in chemical-induced protein aggregation, protein solutions of insulin (0.8 mg/ml) and lysozyme (1 mg/ml) in 10 mM PBS (pH 7.4) were incubated at 37˚C with 20 mM DTT. For the heat-induced aggregation, a 0.25 μM citrate synthase protein was prepared in 50 mM HEPES buffer (pH 8) and incubated with HMGB1 proteins for 1.5 h at 43˚C in the presence or absence of HMGB1 in a thermostatic cell holder. Absorbance was monitored at 320 nm with a Beckman spectrophotometer (Beckman Coulter).

In vivo refolding assay

Chinese hamster lung fibroblast O23 cells were transiently transfected with luciferase plasmid of pRSVLL/V and HMGB1 plasmid (31, 34). pRSVLL/V encoding cytoplasmic luciferase plasmid (a kind gift from Dr. Harm H. Kampinga, University of Groningen, Groningen, The Netherlands) was used for intracytoplasmic protein refolding measurement after heat-shock treatment (34). The cells were split into 24-well plates 24 h after transfection and further incubated at 37˚C for 24 h. The plates were treated with cycloheximide (20 μg/ml) for 30 min, heat-shock treated at 43˚C for 30 min, washed three times with PBS, and then lysed to measure change in luciferase activity. Luciferase activity per microgram protein was measured following the manufacturer's protocol of the Dual luciferase reporter assay system (Promega). pcDNA and pCMV-HSP70 was transfected as negative and positive controls, respectively, for chaperonic function.

Treatment of reactive oxygen species scavengers

To investigate the influence of reactive oxygen species (ROS) generated by polyQ aggregates on the cytoplasmic translocation of HMGB1 protein, we pretreated SHSY5Y cells with ROS scavengers and subsequently compared the number of cells that contained cytoplasmic HMGB1 protein. SHSY5Y cells were pretreated with 10 mM *N*-acetyl-L-cysteine (NAC; Sigma-Aldrich) and 25 nM Mito-TEMPO (Enzo Life Sciences) 1 h before 97Q-GFP transfection. After 48 h of 97Q-GFP transfection, endogenous HMGB1 was immunostained with anti-HMGB1 Ab (Abcam), and cytoplasmic HMGB1 proteins were observed by confocal microscopy (Olympus). We counted 100 GFP-positive cells in multiple random visual fields in each condition and compared the number of cells that contained cytoplasmic HMGB1.

Western blot analysis

To detect protein expression, cells were lysed using Proprep protein extraction solution (Intron) including a mixture of protease inhibitors (Sigma-Aldrich). Certain amounts of protein samples were loaded on 12% SDS-PAGE and transferred to a nitrocellulose membrane. A Western blot analysis was performed using primary Abs of rabbit anti-HMGB1 (Abcam), mouse anti-firefly luciferase (Abcam), and mouse anti-GFP (Santa Cruz Biotechnology), as well as secondary Abs of HRP-labeled goat anti-rabbit and goat anti-mouse Ig (The Jackson Laboratory). ECL was used to reveal the signals (Pierce, Rockford, IL). Relative band intensities were measured using the Image J program (National Institutes of Health).

Immunoprecipitation

To identify the binding of HMGB1 with 25Q- or 97Q-GFP, cells were transiently cotransfected with the indicated plasmids of 25Q- or 97Q-GFP and HMGB1-Myc. Lysed cell homogenates were centrifuged at 13,000 rpm for 15 min and precleared by incubation with protein G-Sepharose (Sigma-Aldrich) at 4˚C for 1 h. The precleared extracts were incubated with mouse anti-GFP Ab (Abcam) overnight and then incubated with protein G-Sepharose for 2 h at 4˚C. Immune complexes were collected by centrifugation and washed with cold PBS. Collected complexes were fractionated by SDS-PAGE, and an immunoblot analysis was performed.

Immunofluorescence and confocal imaging

Cells were cultured in four chambers (Nunc) and fixed with 4% paraformaldehyde in PHEM buffer (60 mM PIPES, 25 mM HEPES, 10 mM EGTA, and 4 mM $MgSO_4$ [pH 7]) for 20 min at room temperature (RT). After fixation, cells were washed three times with cold PBS and permeabilized with 0.2% Triton X-100 and then blocked with 1% BSA-PBS for 1 h at RT. A primary Ab was added in 1% BSA-PBS and incubated overnight at 4˚C. The cells were washed three times with cold PBS, and Alexa 488- or Alexa 594-conjugated secondary Ab (Invitrogen) was added to the cells for 1 h at RT. The cells were washed three times with cold PBS, mounted with Vectashield mounting solution (Vector Laboratories, Burlingame, CA), and observed under a FV1000 confocal microscope (Olympus).

Cell-viability measurement

Cell viability was performed to measure the cytotoxicity induced by 97Q-GFP plasmid overexpression. Briefly, cells at a density of 5×10^3 cells/well were cultured in a 96-well plate, and CCK-8 reagent was added to each well and incubated for 2 h at 37˚C. Cell viability was evaluated by measuring absorbance at 450 nm. For propidium iodide (PI) staining, PI solution was added to culture slide for 20 min at 37˚C followed by washing with PBS. Trypan blue staining was performed by mixing equal volumes of trypan blue and cell suspension. Trypan blue–staining positive cells were counted 48 h after transfection.

Filter trap assay

SHSY5Y cells were overexpressed with a construct of 97Q-GFP for 48 h in the presence of HMGB1 or control plasmids. Cells were sonicated in 100 μl PBS containing 1 mM PMSF, and the cell lysates were harvested after centrifugation. A total of 200 μg proteins were taken and filtered through a 0.22-μm cellulose acetate membrane. The membrane was pre-equilibrated with PBS containing 1% SDS. A dot blotter apparatus (Millipore) was used for the application of samples. After samples were passed through the membrane, the membrane was washed twice with PBS containing 1% SDS buffer. Then, the membrane was immunoblotted with an anti-GFP Ab.

Proximity ligation assay

Molecular interaction was evaluated with the aid of a Duolink Proximity Ligation Assay (PLA) kit (Olink Bioscience). Briefly, cells were cultured in four chambers (Nunc) and fixed with 4% paraformaldehyde in PHEM buffer (60 mM PIPES, 25 mM HEPES, 10 mM EGTA, and 4 mM $MgSO_4$) for 20 min at RT. After fixation, cells were washed three times with cold PBS and incubated with a blocking agent for 1 h. Primary Abs against HMGB1 and GFP were then added, allowed to incubate overnight, and subsequently washed three times (washing buffer: 150 mM NaCl, 1 mM Tris base, and 0.05% Tween 20 [pH 7.4]). Duolink PLA probes were applied and incubated for 1 h in a humidity chamber at 37˚C. Unbound Duolink PLA probes were removed with wash buffer, and the samples were incubated in the ligation solution for 1 h. For amplification, diluted polymerase was applied for 100 min, and the amplified probe was detected with diluted Duolink Detection stock. Images were taken by confocal microscopy.

Mouse embryonic primary striatal neuron cells

Mouse embryonic primary striatal neuron cells were prepared from embryonic day 14. Dissociated striatal neurons were plated at a density of 3.5 hemispheres/10 ml media onto poly-D-lysine– (100 μg/ml) and laminin-coated (100 μg/ml) plates. The cultures were maintained with antibiotics in Neurobasal medium (Life Technologies) supplemented with B27 (Invitrogen). The cells were used for transfection after 7 d of culture. Protocols were reviewed and approved by the Institutional Animal Care and Use Committee of the Yonsei Laboratory Animal Research Center (2010-0392).

Statistics

Statistical analysis was performed by ANOVA followed by the Bonferroni test or Student *t* test. All data were presented as means ± SE.

Results

HMGB1 reduces physical stress–induced protein denaturation in vitro and heat shock–induced luciferase inactivation in O23 cells

To investigate whether HMGB1 exhibits any chaperone-like activity, the ability to prevent chemical- and heat shock–induced target protein aggregations was evaluated by measuring turbidity in vitro. Insulin and lysozyme were used for the chemical (DTT)-induced aggregation. Insulin and lysozyme in 10 mM phosphate (pH 7.4) were incubated with 20 mM DTT in the presence or absence of HMGB1 at 37˚C for the indicated time, and the degree of light scattering by aggregation was measured. As shown in Fig. 1A1 and 1A2, DTT-induced aggregations of both insulin and lysozyme were increased with time; however, the levels of aggregation decreased with the addition of HMGB1. In the heat shock–induced protein aggregation experiments, citrate synthase was used to incubate with HMGB1 protein at 43˚C because citrate synthase is sensitive to thermal treatment >45˚C (35), and HMGB1 protein became turbid when it was heat-treated at 50˚C (Fig. 1B1). Thermally induced aggregation of citrate synthase was significantly reduced with the addition of HMGB1 (Fig. 1B2, 1B3).

Chinese hamster O23 cells were used as a model for determining in vivo refolding assay for intracellular chaperone-like function using luciferase (34). O23 cells were transiently cotransfected with luciferase plasmid with CMV-myc, HMGB1-myc, or HSP70-myc plasmid. CMV-myc and HSP70 plasmids were cotransfected as negative and positive controls, respectively (Fig. 1C). Luciferase activity after thermal stress at 43˚C for 30 min was measured by measuring light absorbance. When O23 cells were cotransfected with luciferase and HMGB1 plasmids, luciferase activity from direct thermal stress was increased compared with the controls.

Overexpression of 97Q-GFP induces nucleocytoplasmic translocation of HMGB1, and cytoplasmic HMGB1 colocalizes to 97Q-GFP

To investigate the effect of HMGB1 on protein aggregation, we introduced an aggregation-prone model of expanded polyQ in SHSY5Y neuroblastoma cell line. The aggregation of the mHtt protein of expanded polyQ results in neuronal cell toxicity, and the clearance of aggregates is considered as a main therapeutic target in Huntington disease. We first tested the aggregate formation of 97Q-GFP in SHSY5Y cells (Supplemental Fig. 1A). When SHSY5Y cells were transfected with the 97Q-GFP construct, distinct aggregates could be observed after 48 h, but this was rare in 25Q-GFP. For 97Q-GFP–transfected cells, nucleocytoplasmic translocation of HMGB1 was clearly observed in confocal microscopy and Western blot analysis of cytosolic fraction of transfected cells (Supplemental Fig. 1A, 1B). We observed that the individual vector of 25Q- and 97Q-GFP expressed well, and the level was not reduced by HMGB1 overexpression (Supplemental Fig. 1C). Aggregation of a fragment of the Htt protein directly causes free radical production in vivo (36), and oxidative potential is important for the nucleocytoplasmic translocation of HMGB1 (11). To test whether ROS scavenging inhibits the translocation of HMGB1, NAC, a precursor of glutathione that acts as a scavenger for the OH radical, and Mito-tempo, a mitochondria-targeted

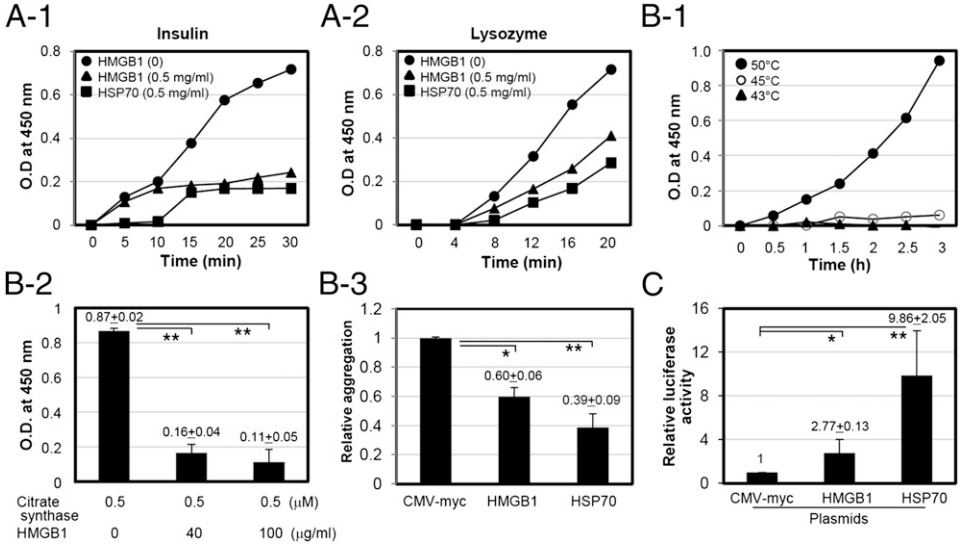

FIGURE 1. HMGB1 protein suppresses chemical- and heat-induced aggregation of target proteins. (**A**) Aggregation curve of insulin [0.8 mg/ml (A-**1**)] and lysozyme [1 mg/ml (A-**2**)] in the absence of HMGB1 (circles) and in the presence of HMGB1 (0.5 mg/ml; triangles) or HSP70 (0.5 mg/ml; squares) induced by 20 mM DTT. (**B-1**) Aggregation of HMGB1 protein by heat treatment. rHMGB1 protein (0.5 mg/ml) was incubated at different temperatures for 3 h, and the aggregation was measured by OD at 340 nm. (**B-2** and **B-3**) Thermal aggregation of citrate synthase. Citrate synthase (0.25 μM) was incubated at 43˚C for 90 min with 0.4 μM of HMGB1 protein. Same molecular concentration of HSP70 protein was used as a positive control. (**C**) O23 cells were transiently cotransfected with luciferase and HMGB1 plasmids. HSP70 plasmid and empty vector pcDNA were used as positive and negative controls, respectively. Cells were treated with cycloheximide for 30 min after 24 h of incubation and heat-shock treated for 30 min at 43˚C to inactivate luciferase. $*p < 0.05$, $**p < 0.01$ versus CMV-myc control ($n = 3$).

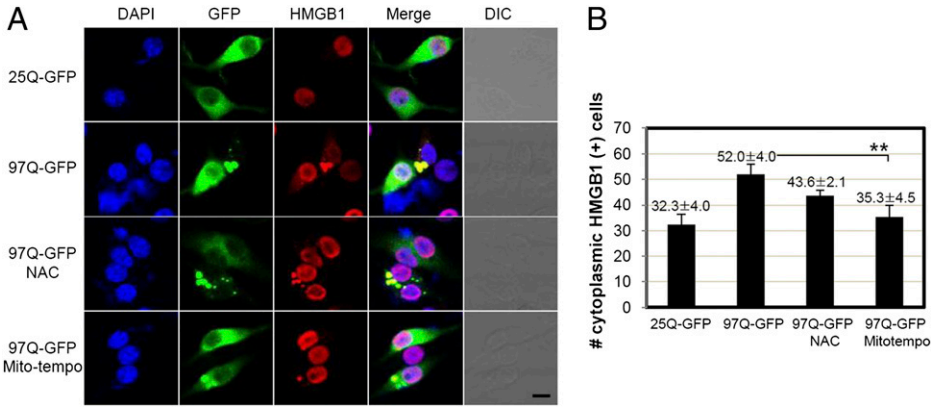

FIGURE 2. ROS generation by 97Q-GFP overexpression induces HMGB1 translocation. (**A**) SHSY5Y cells were transfected with 25Q-GFP or 97Q-GFP plasmid and incubated for 48 h. HMGB1 was immunostained with anti-HMGB1 Ab and Alexa 594–conjugated secondary Ab. Antioxidants NAC (10 mM) and Mito-tempo (25 nM) were applied 1 h before transfection, and endogenous HMGB1 was immunostained to compare degrees of translocation. Scale bar, 10 μm. (**B**) The number of cytoplasmic HMGB1-positive cells was counted. $^{**}p < 0.01$ versus 97Q-GFP ($n = 3$). DIC, Differential interference contrast.

antioxidant with superoxide and alkyl radical–scavenging properties, were treated. As shown in Fig. 2A and 2B, NAC and Mito-tempo scavenging of ROS generated from overexpressed 97Q-GFP aggregates decreased the translocation of HMGB1.

To observe whether HMGB1 directly interact with 97Q-GFP, SHSY5Y cells were overexpressed with 97Q-GFP and immunostained with anti-HMGB1 Ab. Aggregates of 97Q-GFP were colocalized with HMGB1, which were translocated to the cytoplasm (Fig. 3A). The direct interactions between HMGB1 and 97Q-GFP or 25Q-GFP were also shown by immunoprecipitation assay in SHSY5Y and HEK 293 cells (Fig. 3B). To confirm again the interaction, SHSY5Y cells were overexpressed with 97Q-GFP, and Duolink PLA was performed. As shown in Fig. 3C, colocalization of endogenous HMGB1 protein with 97Q-GFP was observed in confocal microscopic analysis. When we investigated the bindings of A and B domains of HMGB1 to 97Q-GFP

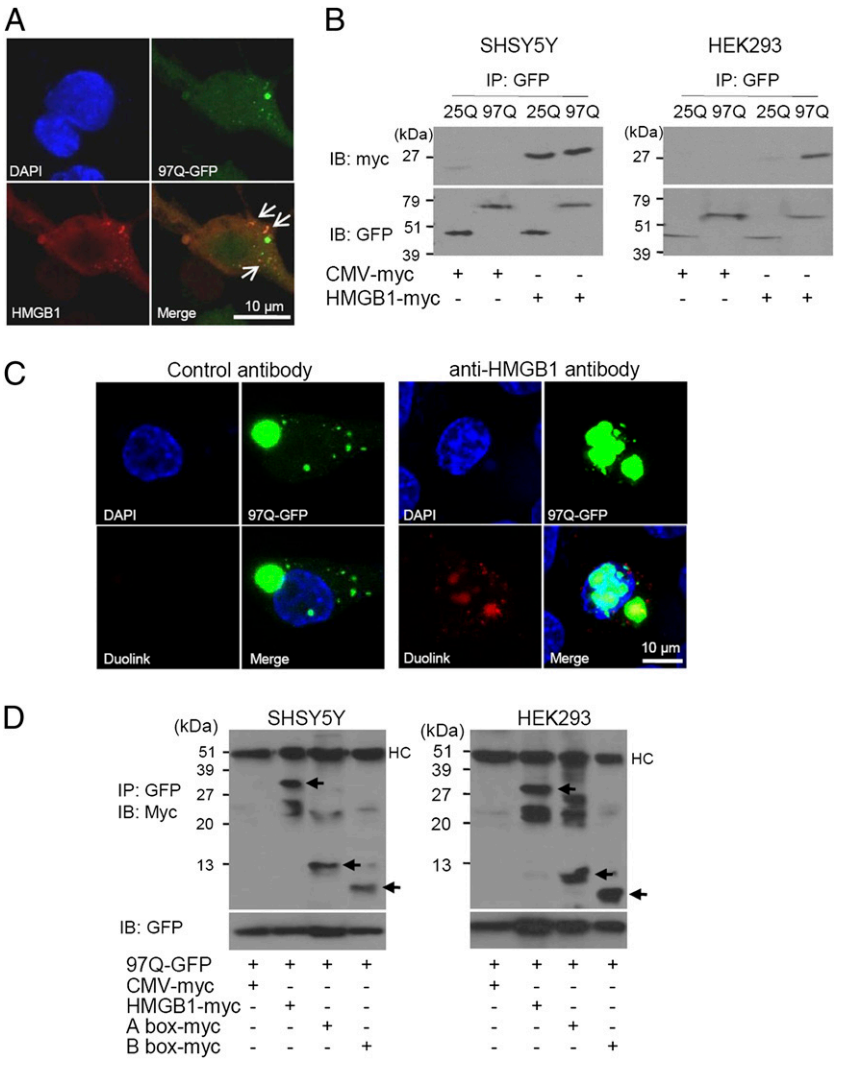

FIGURE 3. Interaction of HMGB1 with 97Q-GFP. (**A**) Confocal analysis for colocalization of HMGB1 with 97Q-GFP. SHSY5Y cells were transfected with 97Q-GFP and immunostained with anti-HMGB1 Ab to observe the colocalization of 97Q-GFP with endogenous HMGB1 protein. (**B**) SHSY5Y and HEK293 cells were cotransfected with 25Q-GFP or 97Q-GFP and HMGB1-myc plasmids, and the cell lysates were immunoprecipitated with anti-GFP Ab followed by immunoblotting with anti-myc Ab to detect HMGB1. CMV-myc was used as a control plasmid. (**C**) Duolink PLA. SHSY5Y cells were transfected with 97Q-GFP, and PLA was performed to observe the colocalization of 97Q-GFP with endogenous HMGB1 protein. (**D**) Interaction of HMGB1 box proteins A and B with 97Q-GFP. SHSY5Y and HEK 293 cells were transiently cotransfected with 97Q-GFP and each plasmid coding wild-type HMGB1, as well as boxes A and B. CMV-myc was used as a negative control plasmid. The cell lysates were coimmunoprecipitated (IP) with anti-GFP Ab for 97Q, and then immunoblotted (IB) with anti-Myc Ab for various types of HMGB1. Expression of 97Q-GFP protein was examined for loading control. Arrows indicate WT HMGB1 and A and B box proteins from the heavy m.w. HC, H chain.

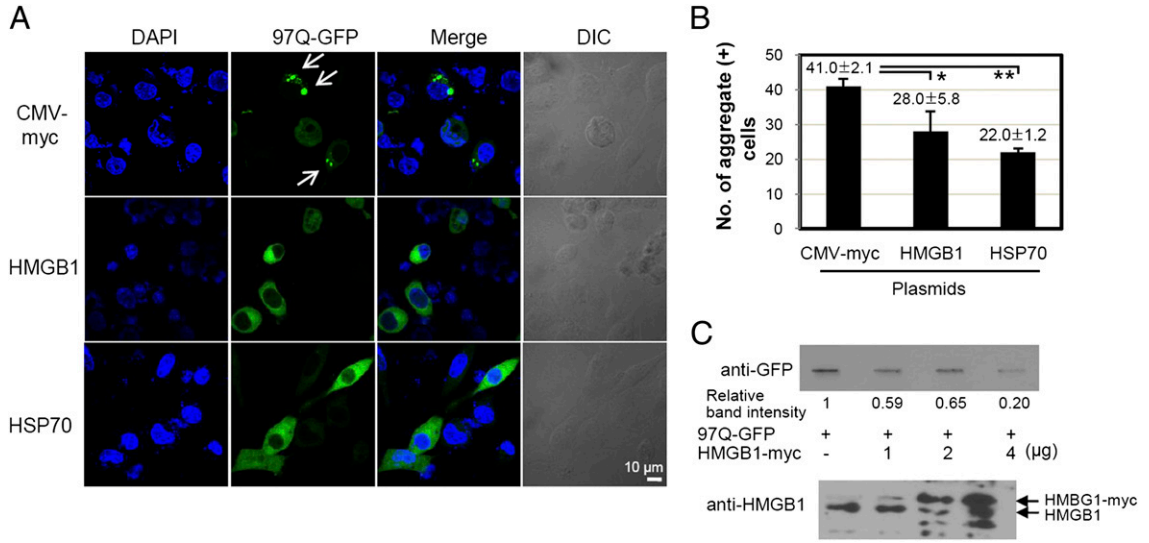

FIGURE 4. HMGB1 reduces the formation of 97Q-GFP aggregates. (**A** and **B**) SHSY5Y cells were cotransfected with 97Q-GFP and HMGB1-myc plasmids and cultured for 48 h. The 97Q-GFP aggregates were analyzed with confocal microscopy, and the numbers of aggregate-positive cells were counted among 100 GFP-positive cells. Arrows indicate 97Q-GFP aggregates. pcDNA and HSP70 plasmids were used as negative and positive controls, respectively. The experiments were repeated three times. (**C**) Analysis of 97Q-GFP aggregates using filter-trap analysis. SHSY5Y cells were cotransfected with a construct of 97Q-GFP and HMGB1, and each cell lysate protein (200 μg) was filtered through a 0.22-μm cellulose acetate membrane for Western blot analysis. Relative band intensities were measured using Image J program (National Institutes of Health). Expression of HMGB1-myc plasmids was observed by Western blot analysis. $*p < 0.05$, $**p = 0.001$ versus CMV-myc control. DIC, Differential interference contrast.

protein, both domains exhibited the binding to 97Q-GFP upon immunoprecipitation analysis using SHSY5Y and HEK293 cells (Fig. 3D).

HMGB1 suppresses the formation of mHtt aggregates

To investigate the effect of HMGB1 on the aggregation of expanded polyQ, SHSY5Y cells were transfected with a construct of 97Q-GFP plasmid and incubated for 48 h in the presence or absence of HMGB1 overexpression (Fig. 4A, 4B). The number of polyQ aggregate-containing cells among 100 GFP-positive cells was significantly reduced when the cells were cotransfected with HMGB1 plasmid. When the amount of aggregates was further analyzed using filter-trap assay, the band intensity showing 97Q-GFP aggregates immobilized on cellulose acetate membrane was decreased in a dose-dependent manner with HMGB1 plasmid transfection (Fig. 4C, *top panel*). The protein expression of

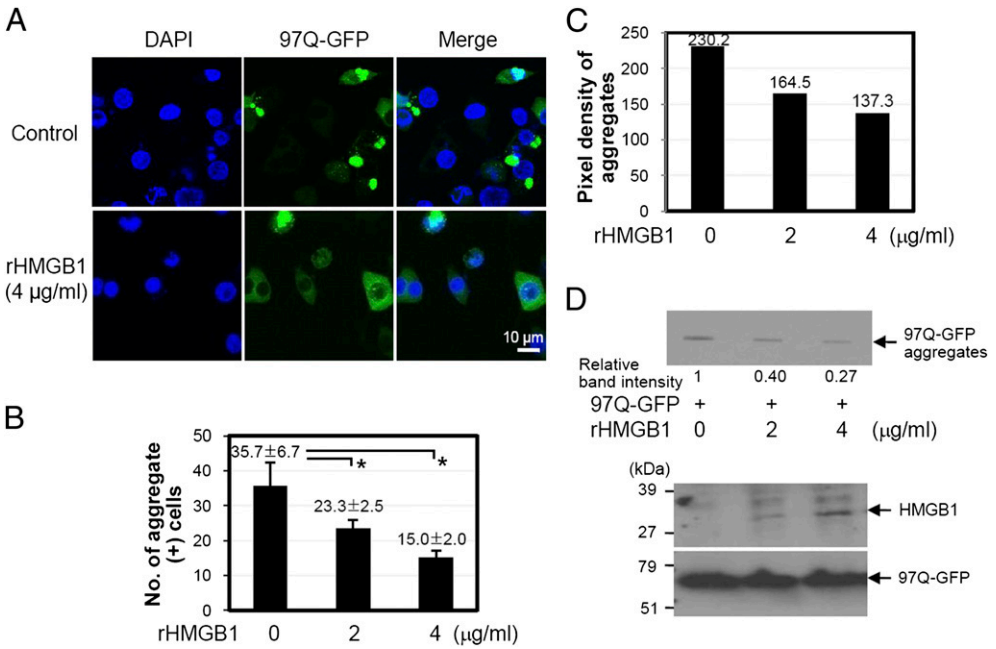

FIGURE 5. Effect of rHMGB1 protein on the formation of 97Q-GFP aggregates. (**A**–**C**) SHSY5Y cells were transiently transfected with 97Q-GFP plasmid and then treated with rHMGB1 at the indicated concentrations. Distribution of 97Q-GFP aggregates was observed (A), and the number of aggregate-containing cells was counted among 100 GFP-positive cells (B). (C) The average pixel density of 30 aggregates was measured after treatment with rHMGB1. (**D**) SHSY5Y cells were transiently transfected with 97Q-GFP plasmid followed by rHMGB1 protein treatment. Cell lysates were analyzed for aggregate formation using filter-trap assay. The filter membrane was immunoblotted with anti-GFP Ab to check the amount of aggregates (*top panel*). Whole-cell lysates for exogenous HMGB1 protein that penetrated the cell membrane was analyzed using anti-His Ab (*bottom panel*). $*p < 0.05$ versus the rHMGB1-untreated group ($n = 3$).

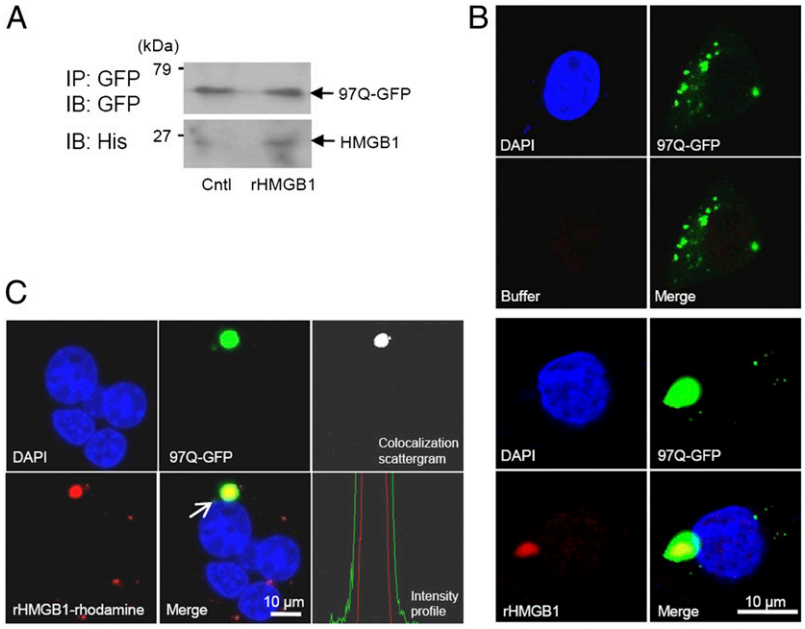

FIGURE 6. Interaction of exogenously treated rHMGB1 with 97Q-GFP. (**A**) SHSY5Y cells were transiently transfected with 97Q-GFP plasmid and then treated with rHMGB protein at 4 μg/ml. SHSY5Y cell lysates were immunoprecipitated (IP) with anti-GFP Ab, and the binding of rHMGB1 protein to 97Q-GFP was observed with anti-His Ab (immunoblot [IB]). (**B**) SHSY5Y cells were transiently transfected with 97Q-GFP plasmid and then treated with rHMGB protein at 4 μg/ml. The cells were immunostained with anti-His Ab for intracellular staining of rHMGB1 protein, which was treated to the cell-culture medium (*bottom panel*). Buffer-treated control is shown in the *upper panel*. (**C**) SHSY5Y cells were transiently transfected with 97Q-GFP and then treated with rhodamine-conjugated rHMGB1 protein at a concentration of 4 μg/ml to detect direct interaction with 97Q-GFP protein. The colocalization of 97Q-GFP and rhodamine-rHMGB1 was observed using colocalization scatter plot and intensity profile analysis, which was measured across the aggregate (arrow). Cntl, Control.

transfected HMGB1 plasmid was observed by Western blot assay (Fig. 4C, *bottom panel*).

Administration of exogenous rHMGB1 protein reduces the formation of mHtt aggregates

Next, we evaluated the effect of exogenous rHMGB1 protein treatment on the cells overexpressing 97Q-GFP, because the addition of exogenous rHMGB1 protein can increase the binding with TLR9 in the cytoplasm (37). We first tested whether exogenous treatment of rHMGB1 protein can penetrate the cell membrane into cytoplasm. Addition of rhodamine-conjugated rHMGB1 proteins to the medium was able to directly penetrate the cell membrane under the observation of confocal microscopy (Supplemental Fig. 2A). This finding was not inhibited by cytochalasin

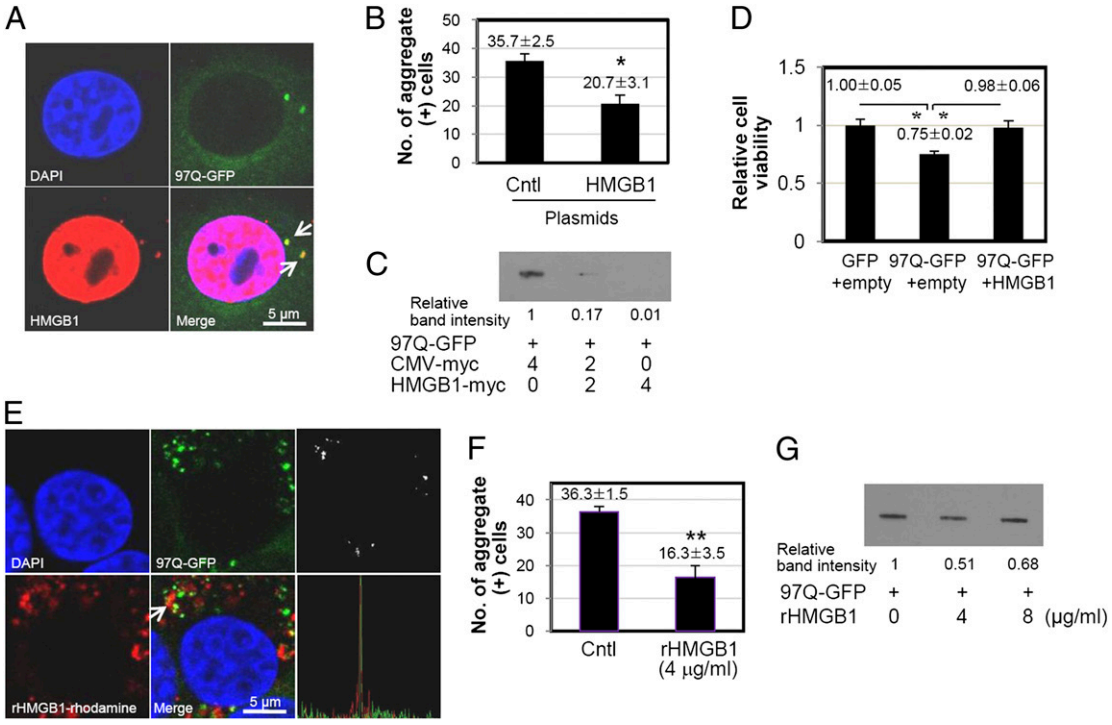

FIGURE 7. Effect of HMGB1 on the formation of 97Q-GFP aggregates in *hmgb1*$^{-/-}$ MEF cells. (**A**–**D**) *Hmgb1*$^{-/-}$ MEF cells were electroporated with a mixture of 97Q-GFP and HMGB1 plasmids, and the colocalization of 97Q-GFP and HMGB1 (arrow) was observed by immunostaining of HMGB1 protein (A). (B) The number of aggregate-containing cells was counted among 100 GFP-positive cells. Filter-trap analysis of whole-cell lysates of *hmgb1*$^{-/-}$ MEF cells, which were cotransfected with 97Q-GFP and HMGB1 plasmids. (C) Relative band intensity was measured. (D) Cell-viability assay was performed 48 h after electroporation. GFP and empty plasmids were used as control plasmids. Cell viability was measured using CCK-8 activity. (**E**–**G**) *Hmgb1*$^{-/-}$ MEF cells were treated with rhodamine-conjugated rHMGB1 protein at 4 μg/ml after the 97Q-GFP overexpression, and the colocalization was observed using colocalization scatter plot and intensity profile analysis (E). (F) The number of aggregate-containing cells was counted among 100 GFP-positive cells. (G) Filter-trap analysis of whole-cell lysates of *hmgb1*$^{-/-}$ MEF cells, which were treated with rHMGB1 protein. *$p < 0.05$ ($n = 3$), **$p < 0.01$ ($n = 3$). Cntl, Control.

B pretreatment, which prevents actin polymerization, even at the high concentration of 50 μg/ml, suggesting that this penetrating mechanism is not relevant with endocytosis. The penetration of rHMGB1 to the cytoplasm was also probed in the cell lysates after cell washing by Western blot analysis (Supplemental Fig. 2B).

When rHMGB1 protein was added to the medium and incubated for 24 h in SHSY5Y cells transfected with 97Q-GFP, the formation of 97Q-GFP aggregates was significantly reduced by rHMGB1 protein treatment (Fig. 5A). The average number of aggregate-containing cells among 100 GFP-positive cells was dose-dependently reduced from 35.7 ± 6.7 to 15.0 ± 2.0 at 4 μg/ml of rHMGB1 protein treatment (Fig. 5B). The average pixel density of 30 aggregates was also reduced by the treatment of rHMGB1 protein (Fig. 5C). In a filter-trap assay, rHMGB1 protein treatment inhibited 97Q-GFP aggregation (Fig. 5D). When SHSY5Y cells were treated with trichostatin A, which is an inhibitor of histone deacetylase, to induce acetylation that results in intracytoplasmic translocation of HMGB1 (38), 97Q-GFP aggregate-positive cells among 100 GFP(+) cells were significantly decreased (Supplemental Fig. 2C, 2D).

We hypothesized that rHMGB1 protein might interact with polyQ directly to reduce the formation of aggregates. The binding of exogenously treated rHMGB1 protein with the aggregates of 97Q-GFP was observed using immunoprecipitation assay (Fig. 6A). 97Q-GFP–overexpressed SHSY5Y cells were treated with 4 μg/ml of His-tagged rHMGB1, and the binding of rHMGB1 to 97Q-GFP could be observed after immmunofluorescence staining of rHMGB1 using anti-His Ab (Fig. 6B). When rhodamine-conjugated rHMGB1 protein was treated to observe direct binding to intracellular 97Q-GFP, colocalization was clearly observed by confocal microscopy (Fig. 6C). Colocalization was confirmed by colocalization scatter plot and cross-sectional intensity profiles provided by confocal microscopy software (Fig. 6C). These data suggest that exogenous rHMGB1 protein enters the cytoplasmic membrane and interacts with polyQ aggregates.

PolyQ aggregates tend to be eliminated by autophagy or lysosomal pathway (21), and HMGB1 is an important autophagy regulator (11). Therefore, we performed PLA to check the possibility that HMGB1-associated aggregates might be localized in autophagosomes. We observed that HMGB1 is colocalized with LC3B, an autophagy marker molecule, and also with some 97Q-GFP aggregates (Supplemental Fig. 3A, 3B).

Effect of HMGB1 on the formation of mHtt aggregates in hmgb1$^{-/-}$ *MEF cells*

Next, we tested the effect of HMGB1 on *hmgb1*$^{-/-}$ MEF cells to confirm that exogenous HMGB1 supplement could assume these functions. When *hmgb1*$^{-/-}$ MEF cells were cotransfected with 97Q-GFP and HMGB1-myc plasmids, the 97Q-GFP protein and its aggregates were observed in the cytoplasm as expected (Fig. 7A). Most of the HMGB1 proteins were observed in the nucleus, because HMGB1 has bipartite nuclear localization signal sequences (38). HMGB1 proteins in the cytoplasm were colocalized with 97Q-GFP aggregates (Fig. 7A). The number of aggregate-positive cells was significantly reduced when HMGB1 is replenished (Fig. 7B), and the production of 97Q-GFP aggregates was decreased in HMGB1-transfected cells on filter-trap analysis (Fig. 7C). 97Q-GFP aggregation decreased cell viability, and cell viability was restored by overexpression of HMGB1 (Fig. 7D).

When *hmgb1*$^{-/-}$ MEF cells transfected with 97Q-GFP were treated with rhodamine-conjugated rHMGB1 protein, the colocalization of HMGB1 and 97Q-GFP was observed, and the number of 97Q-GFP aggregate-containing cells among 100 GFP-positive cells was significantly decreased (Fig. 7E, 7F). The band intensity of filter-trap analysis also decreased after treatment with 4 μg/ml of rHMGB1 (Fig. 7G). rHMGB1 protein treatment at a high

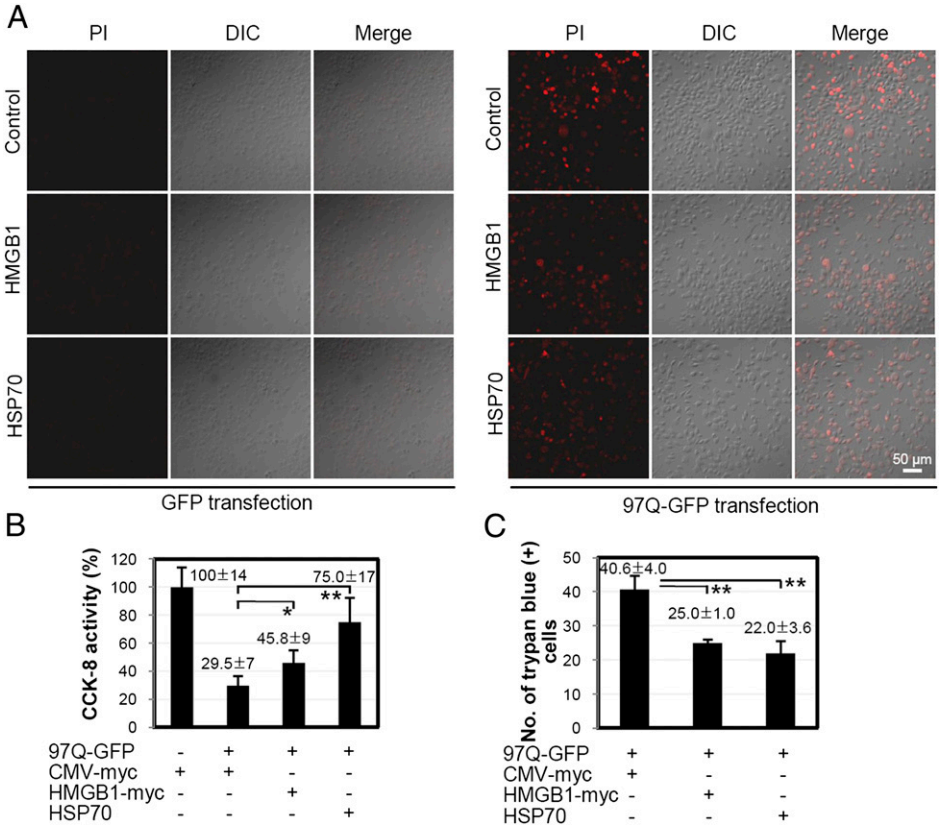

FIGURE 8. Effect of HMGB1 on 97Q-GFP–induced cytotoxicity. SHSY5Y cells were cotransfected with 97Q-GFP plasmid and HMGB1-myc plasmid and incubated for 48 h. GFP transfection was used for a negative control study. Cell viability was measured using PI staining (**A**), CCK-8 activity (**B**), and trypan blue staining (**C**). $*p < 0.05$, $**p < 0.01$ ($n = 3$). DIC, Differential interference contrast.

concentration of 8 μg/ml, however, slightly increased formation of aggregates (Fig. 7G).

Effect of HMGB1 on 97Q-GFP–induced cellular cytotoxicity

We speculated whether the chaperonic activity of HMGB1 could reduce the cellular cytotoxicity caused by the formation of polyQ aggregates. For this, SHSY5Y cells were transiently cotransfected with 97Q-GFP and HMGB1 plasmids for 48 h, after which changes in cell viability were measured. As shown in Fig. 8A, the number of PI-positive cells, indicating cell death, decreased when the cells were cotransfected with HMGB1 plasmid. HSP70 is a well-known chaperonic molecule in Huntington disease and was used as a positive control (39). In the CCK8 cell-viability assay, the cell viability of 97Q-GFP–transfected cells was restored from 29.5 to 45.8% when the cells were cotransfected with HMGB1 plasmid (Fig. 8B). Upon trypan blue staining analysis, which stains dead cells, the transfection of HMGB1 plasmid decreased the number of cell deaths from 40.6 ± 4.0 to 25.0 ± 1.0 (Fig. 8C). These data demonstrate that HMGB1 reduces 97Q-GFP aggregate-induced cell death.

HMGB1 reduces polyQ aggregation in mouse embryonic primary striatal neuron cells

Finally, we used mouse embryonic primary neuronal cells for the chaperone-like activity of HMGB1. For this, mouse embryonic primary striatal neuron cells at embryonic day 14 were isolated and cotransfected with 97Q-GFP in the presence or absence of HMGB1 plasmid. HMGB1 significantly reduced the number of polyQ aggregate-positive cells (Fig. 9A, 9B). The results of the filter-trap analysis showed that the band intensity of 97Q-GFP aggregates was decreased in a dose-dependent manner with HMGB1 (Fig. 9C). HMGB1 protein was colocalized with 97Q-GFP aggregates by confocal microscopy and immunoprecipitation analysis (Fig. 9D, 9E).

When mouse embryonic primary striatal neurons were treated with rHMGB1 protein, the fluorescence intensity of 97Q-GFP was diffusely observed, and the number of polyQ aggregate-positive cells was significantly decreased (Fig. 9F, 9G). The band intensity of filter-trap aggregates showed similar results (Fig. 9H). Treatment of rhodamine-conjugated rHMGB1 protein to primary striatal cells, which were overexpressed with 97Q-GFP, also exhibited HMGB1 binding to 97Q-GFP (Fig. 9I).

Discussion

HMGB1 is a ubiquitous nuclear protein and is diffusely distributed in the cytoplasm, especially of hepatocytes and neuronal cells (40). In various conditions under proinflammatory signals or oxidative stresses, nuclear HMGB1 can be transported into cytoplasm or secreted into the extracellular space. In the nucleus, HMGB1 plays a role as a DNA chaperone that acts as an architectural chromatin-

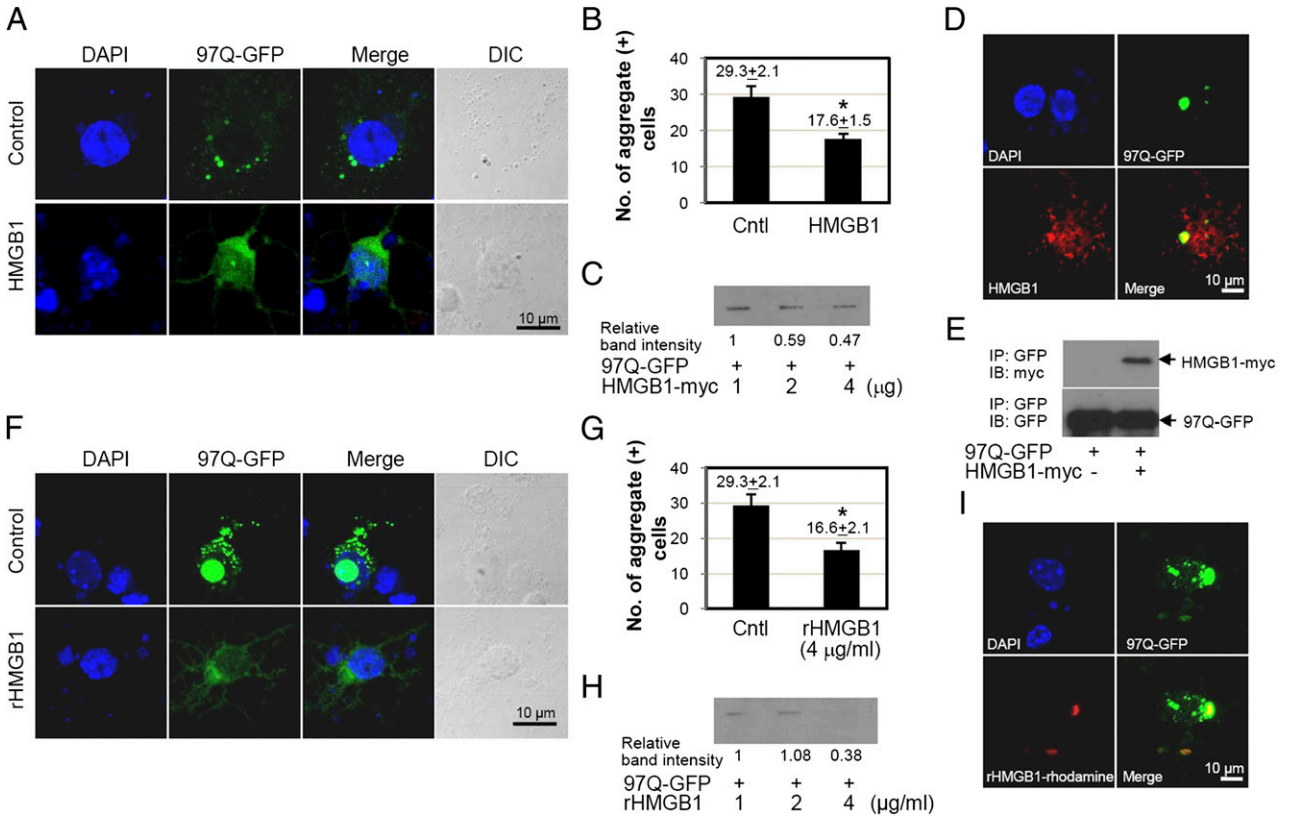

FIGURE 9. Effect of HMGB1 on the formation of 97Q-GFP aggregates in mouse brain primary striatal cells. (**A**–**E**) Mouse embryonic primary striatal neuronal cells were isolated at day 14 and then cotransfected with 97Q-GFP and HMGB1 plasmids. (A) The distribution of 97Q-GFP aggregates was observed under confocal microscopy. (B) The number of aggregate-containing cells was counted among 100 GFP-positive cells. Empty plasmid was used for the control group (Cntl). (C) Filter-trap analysis was performed after cotransfection of 97Q-GFP and HMGB1 plasmids. Colocalization of 97Q-GFP and HMGB1 after cotransfection of both plasmids (D) and immunoprecipitation (IP) analysis (E). (**F**–**H**) Mouse embryonic primary striatal neuronal cells were transfected with 97Q-GFP plasmid for 24 h and then treated with rHMGB1 protein at 4 μg/ml. (F) Distribution of 97Q-GFP aggregates was analyzed by confocal microscopy. (G) The number of aggregate-containing cells was counted among 100 GFP-positive cells. Empty plasmid was used as the control group (Cntl). Filter-trap analysis was performed using the cells that were transfected with 97Q-GFP and incubated with rHMGB1 protein. (**I**) Primary striatal neuronal cells were transfected with 97Q-GFP plasmid, and rhodamine-conjugated rHMGB1 protein was treated. The colocalization of 97Q-GFP with rHMGB1 protein was observed by confocal microscopy. *$p < 0.05$ ($n = 3$). DIC, Differential interference contrast; IB, immunoblotting.

binding factor, which bends DNA and promotes protein assembly at specific DNA targets. Extracellular HMGB1 functions as a proinflammatory cytokine-like molecule by direct binding to TLR4 or indirectly binding with other molecules (41). In addition, HMGB1 can play an intracytoplasmic role as a regulator between macroautophagy and apoptosis (11, 42–44) and a sentinel molecule for viral nucleic acid sensing (45).

In this study, we have demonstrated as a novel finding that HMGB1 exhibits a chaperone-like activity. Extracellular HMGB1 protein reduced protein aggregation induced by heat or chemical stress, and this chaperone-like function could be observed in the cytoplasm by the restoration of intracytoplasmic luciferase activity after heat stress. In addition, HMGB1 was able to reduce the formation of aggregation of expanded polyQ and restore the cell viability from aggregation-induced toxicity. Expanded polyQ is a shared feature of all polyQ diseases, forming misfolded proteins that disrupt normal cellular pathways. Compensatory expression of HMGBs ameliorates polyQ-induced pathology of activation of Chk1 and H2AX, cell-cycle checkpoint kinase and histone that marks sites of DNA structural damage, respectively, and in vivo toxicity of mutant polyQ protein by suppressing genotoxic stress in a *Drosophila* polyQ model (46). On the contrary, the positive interaction of HMGB1 to normal 25Q protein in our result did not agree with a previous report of negative binding to 20Q protein (46). It is possibly due to the number difference of glutamine repeats, 20 or 25, but the clear comparison experiment is necessary to further investigate the physiological meaning of HMGB1 binding to normal polyQ. Classical chaperone proteins of HSP70 and HSP40 family proteins bind to soluble mHtt and suppress aggregation formation and cellular toxicity by correcting the structure of misfolded proteins or degradation of irreversibly damaged polypeptides (47). HSP70 increases the level of soluble polyQ proteins by directly associating with polyQ aggregates in a dynamic and transient manner (48, 49), and HSP40 (DNAJ) associates with aggregates and suppresses aggregation by chaperone modification of high m.w. complexes (29).

Expansion of polyQ repeats leads to early increase of ROS coinciding with polyQ aggregation. Aggregation of a fragment of Htt protein directly causes free radical production in vivo (36), and inhibition of polyQ aggregation suppresses ROS (50, 51). Oxidative potential is important for the nucleocytoplasmic translocation of HMGB1, and redox status of HMGB1 also affects its specific function (52). In our study, ROS generated by overexpression of 97Q-GFP induced translocation of nuclear HMGB1. This translocation was decreased by treatment of ROS scavengers NAC and Mito-tempo, demonstrating the important role of ROS in HMGB1 translocation and binding to expanded polyQ. Our previous finding shows that posttranslational modification of phosphorylation is also responsible for the nucleocytoplasmic transport of HMGB1, and Ca^{2+}-dependent classical protein kinase C is an effector kinase of HMGB1 phosphorylation (53). Considering that expanded polyQ expression induces Ca^{2+}-dependent protein kinase C via metabotropic glutamate receptor–mediated cell signaling (54), it is possible that members of the classical protein kinase C enzyme (α, βI, βII, and γ) family are the main kinases for nucleocytoplasmic transport of HMGB1 to interact with polyQ. Further investigation is necessary to determine whether phosphorylation of HMGB1 could be induced by overexpression of expanded polyQ.

Exogenous administration of rHMGB1 proteins reduced the formation of intracellular mHtt aggregates. The penetration mechanism of rHMGB1 protein into the cytoplasm is not clear, and this penetration was not inhibited by cytochalasin B, suggesting a phagocytosis-independent mechanism. Previous reports that addition of exogenous rHMGB1 proteins to the medium can increase the binding with TLR9 in the cytoplasm (37) and HMGB1–oligodeoxynucleotide complexes are efficiently taken by cells in the absence of HMGB1 receptor of receptor for advanced glycation end products support intracellular uptake of exogenous HMGB1 protein. In HSP70 protein, it can also enter human motor neurons in time- and dose-dependent manners (39, 55) and protect motor neurons subjected to the oxidative stress by decreasing aggregate-positive cells (56, 57), although the mechanism has not been clearly explained.

Overexpression of HMGB1, however, is not always beneficial to reducing polyQ aggregation. A high concentration of HMGB1 rather aggravated the formation of mHtt aggregates in both HMGB1-overexpressed cells and exogenously rHMGB1-treated cell-culture conditions (data not shown). HMGB1 proteins tended to be oligomerized or aggregated by themselves under oxidative stress conditions (data not shown). Excessive amount of HMGB1 is possibly coaggregated with polyQ aggregates. HSP70 protein also showed a similar effect when the protein was overexpressed, suggesting that the optimal concentration of chaperonic proteins is beneficial for the survival of motor neurons (58). The experiments of addition of HMGB1 in *hmgb1*$^{-/-}$ MEF cells and primary neuronal cells confirmed that HMGB1 has a chaperone-like activity.

In summary, we identified a new role of HMGB1 as a chaperone-like molecule in vitro and in vivo. Additionally, the chaperone-like activity of HMGB1 could be a new therapeutic choice of polyQ diseases.

Disclosures

The authors have no financial conflicts of interest.

References

1. Goodwin, G. H., C. Sanders, and E. W. Johns. 1973. A new group of chromatin-associated proteins with a high content of acidic and basic amino acids. *Eur. J. Biochem.* 38: 14–19.
2. Lotze, M. T., and K. J. Tracey. 2005. High-mobility group box 1 protein (HMGB1): nuclear weapon in the immune arsenal. *Nat. Rev. Immunol.* 5: 331–342.
3. Einck, L., and M. Bustin. 1985. The intracellular distribution and function of the high mobility group chromosomal proteins. *Exp. Cell Res.* 156: 295–310.
4. Scaffidi, P., T. Misteli, and M. E. Bianchi. 2002. Release of chromatin protein HMGB1 by necrotic cells triggers inflammation. *Nature* 418: 191–195.
5. Hori, O., J. Brett, T. Slattery, R. Cao, J. Zhang, J. X. Chen, M. Nagashima, E. R. Lundh, S. Vijay, D. Nitecki, et al. 1995. The receptor for advanced glycation end products (RAGE) is a cellular binding site for amphoterin. Mediation of neurite outgrowth and co-expression of rage and amphoterin in the developing nervous system. *J. Biol. Chem.* 270: 25752–25761.
6. Park, J. S., D. Svetkauskaite, Q. He, J. Y. Kim, D. Strassheim, A. Ishizaka, and E. Abraham. 2004. Involvement of toll-like receptors 2 and 4 in cellular activation by high mobility group box 1 protein. *J. Biol. Chem.* 279: 7370–7377.
7. Ombrellino, M., H. Wang, M. S. Ajemian, A. Talhouk, L. A. Scher, S. G. Friedman, and K. J. Tracey. 1999. Increased serum concentrations of high-mobility-group protein 1 in haemorrhagic shock. *Lancet* 354: 1446–1447.
8. Sundén-Cullberg, J., A. Norrby-Teglund, A. Rouhiainen, H. Rauvala, G. Herman, K. J. Tracey, M. L. Lee, J. Andersson, L. Tokics, and C. J. Treutiger. 2005. Persistent elevation of high mobility group box-1 protein (HMGB1) in patients with severe sepsis and septic shock. *Crit. Care Med.* 33: 564–573.
9. Hatada, T., H. Wada, T. Nobori, K. Okabayashi, K. Maruyama, Y. Abe, S. Uemoto, S. Yamada, and I. Maruyama. 2005. Plasma concentrations and importance of High Mobility Group Box protein in the prognosis of organ failure in patients with disseminated intravascular coagulation. *Thromb. Haemost.* 94: 975–979.
10. Wang, H., O. Bloom, M. Zhang, J. M. Vishnubhakat, M. Ombrellino, J. Che, A. Frazier, H. Yang, S. Ivanova, L. Borovikova, et al. 1999. HMG-1 as a late mediator of endotoxin lethality in mice. *Science* 285: 248–251.
11. Tang, D., R. Kang, K. M. Livesey, C. W. Cheh, A. Farkas, P. Loughran, G. Hoppe, M. E. Bianchi, K. J. Tracey, H. J. Zeh, III, and M. T. Lotze. 2010. Endogenous HMGB1 regulates autophagy. *J. Cell Biol.* 190: 881–892.
12. David, D. C., N. Ollikainen, J. C. Trinidad, M. P. Cary, A. L. Burlingame, and C. Kenyon. 2010. Widespread protein aggregation as an inherent part of aging in *C. elegans*. *PLoS Biol.* 8: e1000450.
13. Gidalevitz, T., A. Ben-Zvi, K. H. Ho, H. R. Brignull, and R. I. Morimoto. 2006. Progressive disruption of cellular protein folding in models of polyglutamine diseases. *Science* 311: 1471–1474.

14. Vendruscolo, M. 2012. Proteome folding and aggregation. *Curr. Opin. Struct. Biol.* 22: 138–143.
15. Bjørkøy, G., T. Lamark, A. Brech, H. Outzen, M. Perander, A. Overvatn, H. Stenmark, and T. Johansen. 2005. p62/SQSTM1 forms protein aggregates degraded by autophagy and has a protective effect on huntingtin-induced cell death. *J. Cell Biol.* 171: 603–614.
16. Filimonenko, M., S. Stuffers, C. Raiborg, A. Yamamoto, L. Malerød, E. M. Fisher, A. Isaacs, A. Brech, H. Stenmark, and A. Simonsen. 2007. Functional multivesicular bodies are required for autophagic clearance of protein aggregates associated with neurodegenerative disease. *J. Cell Biol.* 179: 485–500.
17. Moreau, K. L., and J. A. King. 2012. Protein misfolding and aggregation in cataract disease and prospects for prevention. *Trends Mol. Med.* 18: 273–282.
18. Tartaglia, G. G., S. Pechmann, C. M. Dobson, and M. Vendruscolo. 2007. Life on the edge: a link between gene expression levels and aggregation rates of human proteins. *Trends Biochem. Sci.* 32: 204–206.
19. Orr, H. T. 2012. Cell biology of spinocerebellar ataxia. *J. Cell Biol.* 197: 167–177.
20. Penney, J. B., Jr., J. P. Vonsattel, M. E. MacDonald, J. F. Gusella, and R. H. Myers. 1997. CAG repeat number governs the development rate of pathology in Huntington's disease. *Ann. Neurol.* 41: 689–692.
21. Ross, C. A., and M. A. Poirier. 2004. Protein aggregation and neurodegenerative disease. *Nat. Med.* 10(Suppl): S10–S17.
22. Vachharajani, S. N., R. K. Chaudhary, S. Prasad, and I. Roy. 2012. Length of polyglutamine tract affects secondary and tertiary structures of huntingtin protein. *Int. J. Biol. Macromol.* 51: 920–925.
23. Bence, N. F., R. M. Sampat, and R. R. Kopito. 2001. Impairment of the ubiquitin-proteasome system by protein aggregation. *Science* 292: 1552–1555.
24. McCampbell, A., J. P. Taylor, A. A. Taye, J. Robitschek, M. Li, J. Walcott, D. Merry, Y. Chai, H. Paulson, G. Sobue, and K. H. Fischbeck. 2000. CREB-binding protein sequestration by expanded polyglutamine. *Hum. Mol. Genet.* 9: 2197–2202.
25. Hartl, F. U., A. Bracher, and M. Hayer-Hartl. 2011. Molecular chaperones in protein folding and proteostasis. *Nature* 475: 324–332.
26. Hageman, J., M. A. van Waarde, A. Zylicz, D. Walerych, and H. H. Kampinga. 2011. The diverse members of the mammalian HSP70 machine show distinct chaperone-like activities. *Biochem. J.* 435: 127–142.
27. Turturici, G., G. Sconzo, and F. Geraci. 2011. Hsp70 and its molecular role in nervous system diseases. *Biochem. Res. Int.* 2011: 618127.
28. Yamagishi, N., K. Goto, S. Nakagawa, Y. Saito, and T. Hatayama. 2010. Hsp105 reduces the protein aggregation and cytotoxicity by expanded-polyglutamine proteins through the induction of Hsp70. *Exp. Cell Res.* 316: 2424–2433.
29. Labbadia, J., S. S. Novoselov, J. S. Bett, A. Weiss, P. Paganetti, G. P. Bates, and M. E. Cheetham. 2012. Suppression of protein aggregation by chaperone modification of high molecular weight complexes. *Brain* 135: 1180–1196.
30. Sellamuthu, S., B. H. Shin, H. E. Han, S. M. Park, H. J. Oh, S. H. Rho, Y. J. Lee, and W. J. Park. 2011. An engineered viral protease exhibiting substrate specificity for a polyglutamine stretch prevents polyglutamine-induced neuronal cell death. *PLoS ONE* 6: e22554.
31. Youn, J. H., and J. S. Shin. 2006. Nucleocytoplasmic shuttling of HMGB1 is regulated by phosphorylation that redirects it toward secretion. *J. Immunol.* 177: 7889–7897.
32. Youn, J. H., Y. J. Oh, E. S. Kim, J. E. Choi, and J. S. Shin. 2008. High mobility group box 1 protein binding to lipopolysaccharide facilitates transfer of lipopolysaccharide to CD14 and enhances lipopolysaccharide-mediated TNF-α production in human monocytes. *J. Immunol.* 180: 5067–5074.
33. Horwitz, J., M. Bova, Q. L. Huang, L. Ding, O. Yaron, and S. Lowman. 1998. Mutation of alpha B-crystallin: effects on chaperone-like activity. *Int. J. Biol. Macromol.* 22: 263–269.
34. Nollen, E. A., A. E. Kabakov, J. F. Brunsting, B. Kanon, J. Höhfeld, and H. H. Kampinga. 2001. Modulation of in vivo HSP70 chaperone activity by Hip and Bag-1. *J. Biol. Chem.* 276: 4677–4682.
35. Sbroggiò, M., R. Ferretti, E. Percivalle, M. Gutkowska, A. Zylicz, W. Michowski, J. Kuznicki, F. Accornero, B. Pacchioni, G. Lanfranchi, et al. 2008. The mammalian CHORD-containing protein melusin is a stress response protein interacting with Hsp90 and Sgt1. *FEBS Lett.* 582: 1788–1794.
36. Hands, S., M. U. Sajjad, M. J. Newton, and A. Wyttenbach. 2011. In vitro and in vivo aggregation of a fragment of huntingtin protein directly causes free radical production. *J. Biol. Chem.* 286: 44512–44520.
37. Ivanov, S., A. M. Dragoi, X. Wang, C. Dallacosta, J. Louten, G. Musco, G. Sitia, G. S. Yap, Y. Wan, C. A. Biron, et al. 2007. A novel role for HMGB1 in TLR9-mediated inflammatory responses to CpG-DNA. *Blood* 110: 1970–1981.
38. Bonaldi, T., F. Talamo, P. Scaffidi, D. Ferrera, A. Porto, A. Bachi, A. Rubartelli, A. Agresti, and M. E. Bianchi. 2003. Monocytic cells hyperacetylate chromatin protein HMGB1 to redirect it towards secretion. *EMBO J.* 22: 5551–5560.
39. Novoselova, T. V., B. A. Margulis, S. S. Novoselov, A. M. Sapozhnikov, J. van der Spuy, M. E. Cheetham, and I. V. Guzhova. 2005. Treatment with extracellular HSP70/HSC70 protein can reduce polyglutamine toxicity and aggregation. *J. Neurochem.* 94: 597–606.
40. Bustin, M., and N. K. Neihart. 1979. Antibodies against chromosomal HMG proteins stain the cytoplasm of mammalian cells. *Cell* 16: 181–189.
41. Sims, G. P., D. C. Rowe, S. T. Rietdijk, R. Herbst, and A. J. Coyle. 2010. HMGB1 and RAGE in inflammation and cancer. *Annu. Rev. Immunol.* 28: 367–388.
42. Zhang, Y., Y. Cheng, X. Ren, L. Zhang, K. L. Yap, H. Wu, R. Patel, D. Liu, Z. H. Qin, I. M. Shih, and J. M. Yang. 2012. NAC1 modulates sensitivity of ovarian cancer cells to cisplatin by altering the HMGB1-mediated autophagic response. *Oncogene* 31: 1055–1064.
43. Livesey, K. M., R. Kang, P. Vernon, W. Buchser, P. Loughran, S. C. Watkins, L. Zhang, J. J. Manfredi, H. J. Zeh, III, L. Li, et al. 2012. p53/HMGB1 complexes regulate autophagy and apoptosis. *Cancer Res.* 72: 1996–2005.
44. Kang, R., K. M. Livesey, H. J. Zeh, III, M. T. Lotze, and D. Tang. 2011. Metabolic regulation by HMGB1-mediated autophagy and mitophagy. *Autophagy* 7: 1256–1258.
45. Yanai, H., T. Ban, Z. Wang, M. K. Choi, T. Kawamura, H. Negishi, M. Nakasato, Y. Lu, S. Hangai, R. Koshiba, et al. 2009. HMGB proteins function as universal sentinels for nucleic-acid-mediated innate immune responses. *Nature* 462: 99–103.
46. Qi, M. L., K. Tagawa, Y. Enokido, N. Yoshimura, Y. Wada, K. Watase, S. Ishiura, I. Kanazawa, J. Botas, M. Saitoe, et al. 2007. Proteome analysis of soluble nuclear proteins reveals that HMGB1/2 suppress genotoxic stress in polyglutamine diseases. *Nat. Cell Biol.* 9: 402–414.
47. Jana, N. R., M. Tanaka, G. Wang, and N. Nukina. 2000. Polyglutamine length-dependent interaction of Hsp40 and Hsp70 family chaperones with truncated N-terminal huntingtin: their role in suppression of aggregation and cellular toxicity. *Hum. Mol. Genet.* 9: 2009–2018.
48. Kim, S., E. A. Nollen, K. Kitagawa, V. P. Bindokas, and R. I. Morimoto. 2002. Polyglutamine protein aggregates are dynamic. *Nat. Cell Biol.* 4: 826–831.
49. Rujano, M. A., H. H. Kampinga, and F. A. Salomons. 2007. Modulation of polyglutamine inclusion formation by the Hsp70 chaperone machine. *Exp. Cell Res.* 313: 3568–3578.
50. Bertoni, A., P. Giuliano, M. Galgani, D. Rotoli, L. Ulianich, A. Adornetto, M. R. Santillo, A. Porcellini, and V. E. Avvedimento. 2011. Early and late events induced by polyQ-expanded proteins: identification of a common pathogenic property of polYQ-expanded proteins. *J. Biol. Chem.* 286: 4727–4741.
51. Wyttenbach, A., O. Sauvageot, J. Carmichael, C. Diaz-Latoud, A. P. Arrigo, and D. C. Rubinsztein. 2002. Heat shock protein 27 prevents cellular polyglutamine toxicity and suppresses the increase of reactive oxygen species caused by huntingtin. *Hum. Mol. Genet.* 11: 1137–1151.
52. Tang, D., R. Kang, H. J. Zeh, III, and M. T. Lotze. 2011. High-mobility group box 1, oxidative stress, and disease. *Antioxid. Redox Signal.* 14: 1315–1335.
53. Oh, Y. J., J. H. Youn, Y. Ji, S. E. Lee, K. J. Lim, J. E. Choi, and J. S. Shin. 2009. HMGB1 is phosphorylated by classical protein kinase C and is secreted by a calcium-dependent mechanism. *J. Immunol.* 182: 5800–5809.
54. Ribeiro, F. M., M. Paquet, L. T. Ferreira, T. Cregan, P. Swan, S. P. Cregan, and S. S. Ferguson. 2010. Metabotropic glutamate receptor-mediated cell signaling pathways are altered in a mouse model of Huntington's disease. *J. Neurosci.* 30: 316–324.
55. Tidwell, J. L., L. J. Houenou, and M. Tytell. 2004. Administration of Hsp70 in vivo inhibits motor and sensory neuron degeneration. *Cell Stress Chaperones* 9: 88–98.
56. Guzhova, I. V., A. C. Arnholdt, Z. A. Darieva, A. V. Kinev, E. B. Lasunskaia, K. Nilsson, V. M. Bozhkov, A. P. Voronin, and B. A. Margulis. 1998. Effects of exogenous stress protein 70 on the functional properties of human promonocytes through binding to cell surface and internalization. *Cell Stress Chaperones* 3: 67–77.
57. Guzhova, I., K. Kislyakova, O. Moskaliova, I. Fridlanskaya, M. Tytell, M. Cheetham, and B. Margulis. 2001. In vitro studies show that Hsp70 can be released by glia and that exogenous Hsp70 can enhance neuronal stress tolerance. *Brain Res.* 914: 66–73.
58. Kalmar, B., and L. Greensmith. 2009. Activation of the heat shock response in a primary cellular model of motoneuron neurodegeneration-evidence for neuroprotective and neurotoxic effects. *Cell. Mol. Biol. Lett.* 14: 319–335.